Desalination and Water Treatment
www.deswater.com

doi: 10.5004/dwt.2018.22971

130 (2018) 172–181
October

Selective removal of cadmium ions from water samples by using Br-PADAP functionalized SBA-15 particles

Zahra Khanjari[a], Ali Mirabi[a,*], Ali Shokuhi Rad[b,*], Majid Moradian[a]

[a]*Department of Chemistry, Qaemshahr Branch, Islamic Azad University, Qaemshahr, Iran, email: a.mirabi@qaemiau.ac.ir (A. Mirabi)*
[b]*Department of Chemical Engineering, Qaemshahr Branch, Islamic Azad University, Qaemshahr, Iran*
a.shokuhi@gmail.com, a.shokuhi@qaemiau.ac.ir (A.S. Rad)

Received 6 March 2018; Accepted 13 August 2018

Abstract

The focus of the study is on the optimization of variables influencing the removal of Cd(II) ions using colloidal particles based on 2-(5-bromo-2-pyridylazo)-5-diethylamino phenol (Br-PADAP) functionalized on Mesoporous Santa Barbara Amorphous-15 (SBA-15). The Br-PADAP-functionalized SBA-15 mesoporous silica was synthesized and utilized as an adsorbent for removal of cadmium ions. By means of thermogravimetric analysis, transmission electron microscope, Brunauer, Emmett, and Teller, and CHNS analysis, the structural and physicochemical properties of the SBA-15 and its complex with Br-PADAP were characterized. The effects of different variables such as pH, amount of sorbent, temperature, and contact time on the adsorption of Cd(II) ions were examined. The highest adsorption capacity of the adsorbent was found to be considerable (5,000.0 mg g^{-1}) by using the functionalized material. The reusability of the resulted composite is found for more than six cycles. The negative value of ΔG along with the positive value of ΔH shows that the cadmium adsorption on Br-PADAP/SBA-15 is a spontaneous and endothermic process.

Keywords: Aqueous solutions; Removal of cadmium; SBA-15; Surface modification

1. Introduction

Environmental pollution is a major issue in recent technological development. Heavy metal ion pollution demonstrates a serious threat to human health and ecological systems. Heavy metals such as cadmium ion are hazardous pollutants that affect the physical and chemical properties of water and natural resources [1]. Moreover, cadmium is included on the US Environmental Protection Agency's (EPA) list of priority pollutions [2]. It may exist in water as a hydrated ion, and as inorganic complexes such as carbonates [3]. It can be introduced in water from weathering and erosion of soils, atmospheric deposition, cadmium–nickel batteries, leakage from landfalls, stabilizers for PVC, contaminated sites, the dispersive use of sludge, refined petroleum products, fertilizers in agriculture, and alloys that are the result of industrial activities. It is nonbiodegradable and travels through the food chain. Cadmium is very toxic to animals. The harmful effects of cadmium reported include a number of acute and chronic disorders, such as lung problems, renal damage, emphysema, testicular atrophy, cancer, and hypertension in humans [4,5]. The average daily intake for humans is estimated as 0.15 μg from air and 1 μg from water [6]. In humans, nausea and vomiting have been recorded at levels of 15 mg L^{-1} with no adverse effects at 0.05 mg L^{-1}. Severe toxic, but nonfatal, symptoms are reported at concentrations of 10–326 mg L^{-1} of cadmium [7,8]. Accordingly, expansion of new approaches that simplify the removal of Cd ions from wastewaters is of great important. There are various traditional techniques for the treatment of heavy metal pollution, including chemical precipitation, flocculation/coagulation, membrane separation (ultrafiltration, reverse osmosis), adsorption [9], biosorption [10], catalytic oxidation, and ozonation [11].

* Corresponding author.

Adsorption is widely used in the removal of heavy metals from wastewater by various sorbent compounds, such as polymers [12], zeolites [13], clay minerals [14], oxides [15], graphene oxide [16], biosorbents [17], amorphous silica [18], Fe_3O_4 [19–21], and Al_2O_3 [22]. Nevertheless, some materials suffer from inherent problems [23], such as low removal capacity, low selectivity, long equilibrium time, and mechanical and thermal instability. Recently, mesoporous materials have been paid much attention owing to their scientific importance and great potentials in practical applications such as catalysis [24–26], adsorbents [27], sensors [28], and host materials [29]. Furthermore, comparison with the other silica materials, SBA-15 displays the highest hydrothermal stability [30,31] that is appropriate for any use in aqueous media. SBA-15 functionalized with different function groups have been largely used as adsorbent owing to their high selectivity for ions adsorption [32]. Groups such as carboxylic acid [33], iminoacetate [34], sulfonic acid [35], amino-carboxyl [36], dithizone [37], and amine and thio [38] were immobilized onto different substrates to remove cadmium.

In the study, for the first time, a colloidal solution based on Br-PADAP functionalized SBA-15 nanoparticles was prepared for removal of cadmium ions from wastewater samples using atomic absorption spectrophotometer. The structure of nanoparticles was characterized via different techniques such as transmission electron microscope (TEM), Brunauer, Emmett, and Teller (BET), and thermogravimetric analysis (TGA). Then, the influence of different variables such as pH, initial Cd(II) ion concentration, contact time, and amount of adsorbent on the removal of Cd(II) ion has been investigated. The adsorption rates were evaluated by fitting the experimental data to conventional kinetic models such as first- and second-order as well as intraparticle diffusion models.

2. Experimental

2.1. Reagent and instruments

All materials and solvents were purchased from Merck except Plaronic P-123 that purchased from Sigma Aldrich. The analytical grade of nitrate salts of elements (all from Merck) was of the highest purity available and used without any further purification. pH meter model Metrohm 744 was used for pH measurements pH. Kokusan centrifuge model H-11n was used for separation of the nanocomposite. For analysis of cadmium ions, a Thermo M series (Model: M5) flame atomic absorption spectrometer (FAAS) was used. TEM by HF2000, Hitachi high-technologies Europe GmbH, Krefeld model was used to measuring porous size. Surface area was determined by BET technique (Quanta chrome, Chem BET 300 TPR/TPD). CHNS analysis (Costech ECS4010, Italy) and TGA (Bahr thermo analyze) were used to proving Br-PADAP stabilization on the surface of SBA-15. For TGA analysis, all samples were heated from 25°C to 800°C at a rate of 20°C min^{-1} in a nitrogen atmosphere.

2.2. Synthesis of SBA-15 mesoporous silica

To prepare SBA-15, we followed the methodology used in Ref. [39].

2.3. Synthesis of nanocomposites

0.4 g of SBA-15 mesoporous silica was added to 10 mL solution including 0.8 mg SDS and 0.5 mL solution of 0.01 M Br-PADAP. The pH of the solution was adjusted to 2.0 using 1 M HCl solution [40]. The solution was placed within an oil bath at 65°C for 24 h. After that, the modified SBA-15 was filtered off and then it was washed with double distilled water. Then, it was dried at room temperature. After these steps, the Br-PADAP was physically adsorbed onto the surface of SBA-15. UV-vis spectrophotometer was used to provide any proof for Br-PADAP immobilization on SBA-15 nanosorbent. As a result, the absorbance of Br-PADAP in solution decreases after stabilization on SBA-15 nanosorbent.

2.4. General procedure

0.03 g of the prepared nanocomposite was added to the 100 mL of cadmium solution (100 mg L^{-1}) and then 2 mL of ammonia/ammonium chloride buffer solution (1.0×10^{-3} mol L^{-1}, pH 9.0) was added in it. Then, the solution was mixed in a shaker for 90 min that provides cadmium adsorption of the nanocomposite. Subsequently, the solution was centrifuged at 5,000 rpm for 15 min following by measuring the solution absorbance by FAAS at λ = 228.8 nm.

2.5. Adsorption mechanism

Obviously, the electrostatic interactions between Br-PADAP and Cd(II) ions are disgusting under acidic condition, in which on one side, H+ ions are in competition with Cd(II) ions for closing on the adsorbent surfaces, and on the other hand, those ions cause protonation of ligand that repels cadmium ions because of their positive charge. The results reveal that N and O atoms in PADAP involve in the adsorption process by chemical coordination with Cd(II) ions. Therefore, it is suggested that the adsorption process occurs via chemisorption.

Fig. 1. A schematic of SDS–PADAP immobilization onto SBA-15 mesoporous silica surface.

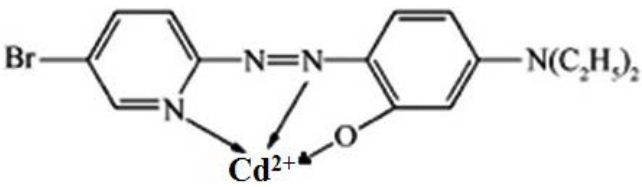

Fig. 2. Scheme of the successive stage of Br-PADAP toward adsorption of cadmium ions.

3. Result and discussion

3.1. Physicochemical properties of SBA-15 and Br-PADAP/SBA-15

Synthesized SBA-15 and Br-PADAP/SBA-15 were characterized by TEM, BET, TGA, and CHNS analyses. Figs. 3(a) and (b) are provided to show side and top views of SBA-15. As shown in Fig. 3(a), all pores are uniformly parallel compared with each other. According to Fig. 3(b), it can be found that the SBA-15 pore size is less than 10 nm having uniformly hexagonal structure.

BET analysis for SBA-15 was performed before and after coating with Br-PADAP ligand. According to the results, 1 g of SBA-15 and Br-PADAP/SBA-15 shows about 329.961 and 287.854 m^2 surfaces, respectively. In fact, this grate enhancement in the surface area of modified SBA-15 causes more sites for adsorption of Cd(II) ions.

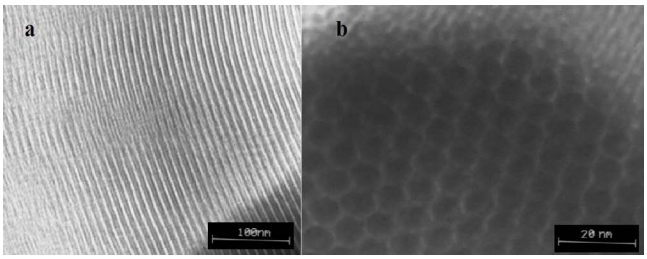

Fig. 3. TEM image of SBA-15 in side view (a) and top view (b).

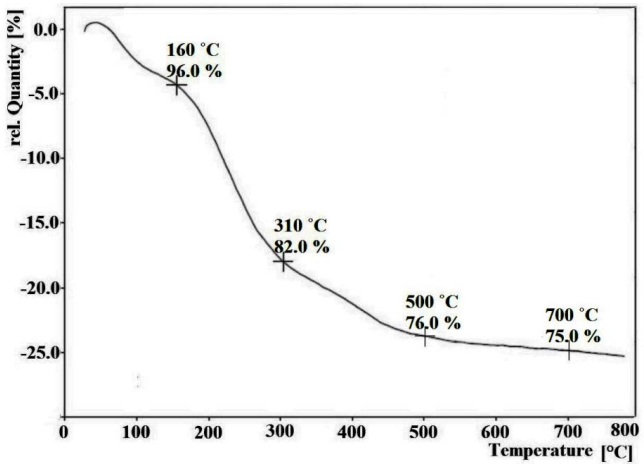

Fig. 4. Thermogravimetric analysis (TGA) curve of Br-PADAP/SBA-15 with a heating rate of 10°C min^{-1}.

To finding the thermal stability of modified SBA-15 and the presence of the organic group, TGA analysis was used (Fig. 4). The weight loss <5% at around 160°C and between 160°C and 500°C (20.0%) are due to the desorbed water and Br-PADAP ligand on the modified SBA-15, respectively. At $T > 500$°C, a small slop of weight loss is observed continually, which could be related to the combustion of remaining organic material.

Elemental analysis CHNS was used to identify the types of elements in Br-PADAP/SBA-15 and it can be used to determine the ratio of elements in the sample material.

As shown in Table 1, the presence of nitrogen and carbon in CHNS analysis of nanocomposite, confirms the presence of Br-PADAP ligand on the surface of SBA-15.

3.2. Optimization of adsorption conditions

To get a high Cd ions removal percent, the impact of various parameters, such as pH, amount of sorbent, contact time, and the temperature, was optimized. In all optimization steps, the concentration of Cd(II) ions was adjusted at 100 mg L^{-1}.

3.2.1. Effect of pH on adsorption

Fig. 5 shows the effect of pH of the solution on the removal of Cd(II) ions. We found that the Cd(II) ions removal by the adsorbent rises with the increase in the pH and reaches to a maximum at pH 9. The negligible adsorption at low pH values may be accredited to the higher concentration as well as extraordinary mobility of the H^+ that is favorably adsorbed rather than the Cd(II) ions. At high pH values, the existence of H^+ ions is lower. On the other hand, high pH value provides the higher number of ligands with negatives charges; therefore, one can expect better adsorption of Cd(II) ions.

3.2.2. The result of contact time and temperature

Fig. 6 shows the effect of contact time and temperature on the adsorption of Cd(II) ions by Br-PADAP/SBA-15. In this regard, the initial cadmium concentration of 100 mg L^{-1}, pH of 9, and Br-PADAP/SBA-15 dose of 5.0 mg in 100 mL were used. The mixture was agitated in a mechanical shaker for different periods (5–120 min) and different temperatures (25°C, 35°C, and 45°C). The obtained results are summarized in Fig. 6.

These results point to the fast adsorption of Cd(II) ions at first (until 40 min) and the equilibrium was achieved after 90 min. Taking into account these results, a contact time

Table 1
Elemental analysis of Br-PADAP/SBA-15

Reten. time (min)	Response	Weight (g)	Weight (%)	Element name	Carbon response ratio
1.217	2,413.23	0.024	4.80	Nitrogen	0.299
2.153	8,074.25	0.083	16.06	Carbon	1.000
7.972	4,927.00	0.049	9.80	Hydrogen	0.610
17.913	0.05	0.000	0.00	Sulphur	0.000
Sample weight: 0.500 (g)		0.156	30.66		

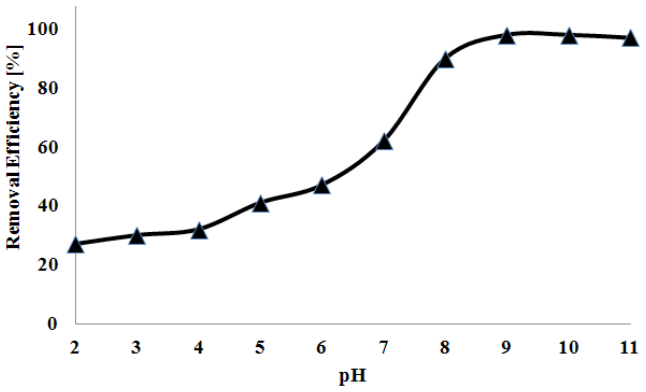

Fig. 5. Effect of pH on the removal of Cd(II) ions.

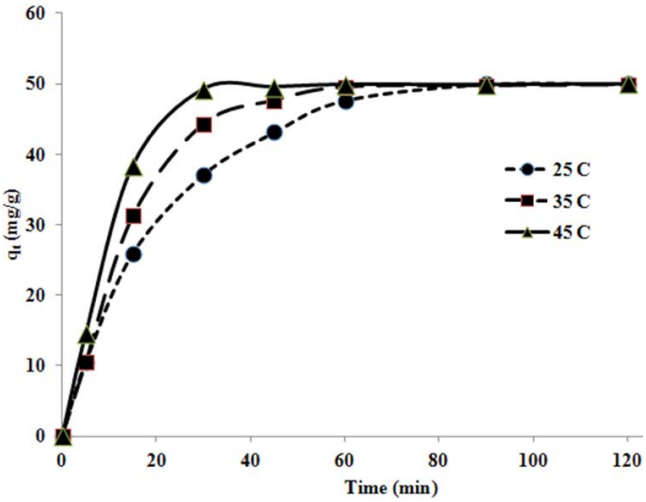

Fig. 6. Effect of contact time and temperature on the removal efficiency with Br-PADAP/SBA-15 (the initial concentration, pH, and the volume of solution and the amount of adsorbent were 100 mg L^{-1}, 9.0, 100 mL, and 30 mg, respectively).

of 90 min was chosen for further experiments. It was also observed that the removal efficiency rises by the increase in the solution temperature that points to the endothermic property of adsorption process.

3.2.3. Effect of sorbent dosage

The optimum amount of the sorbent (SBA-15 and Br-PADAP/SBA-15) for maximum take-up was determined by increasing the amount of sorbent added into 100 mL of 100 mg L^{-1} cadmium ions. Results are provided in Fig. 7. It can be seen from the Fig. 7, the removal of Cd(II) increases by increasing the adsorbent dose in the range from 3 to 30 mg, and finally, the quantitative extraction of cadmium ions (percent of extraction ≥96%) was achieved using 30 mg of sorbent. Further increase in the dose had a negligible effect on the sorption; this increase is because at the higher dose of composite further binding sites are accessible owing to the enlarged surface area. Hence, subsequent removal experiments were done with 30 mg of nanostructure adsorbent for removing of cadmium ions. In

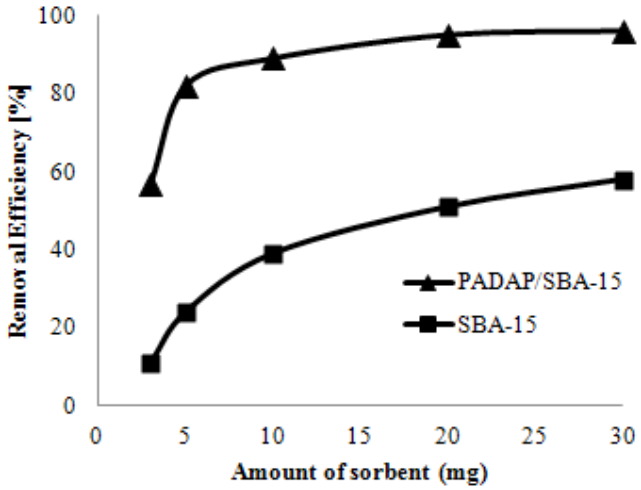

Fig. 7. Effect of different doses of SBA-15 and Br-PADAP/SBA-15 for removal of Cd(II) ions.

addition, SBA-15 did not result in good efficiency when is used separately.

3.3. Effect of electrolyte

Existing irritating species can cause the overlapping and inaccurate removal of cadmium ions. To assay, the effect of interfering ions on the Cd ions adsorption, the NaCl, and Na_2SO_4 salts was introduced to the Cd (II) solution. As the concentration of Na_2SO_4 and NaCl changes from 0.01 to 1.0 M, the Cd (II) removal decreases from 98% to 95% and from 97% to 93%, respectively, using 100 mL of 100 mg L^{-1} Cd(II) solution at pH 9, temperature 25°C, and contacting time of 90 min. The adsorption of sodium ions on the adsorbent surface (due to the negative charge on the adsorbent surface at high pH values) has affected the formation of the cadmium–ligand complex. On the other hand, due to the presence of chloride ions in the solution and the possible formation of the $CdCl_4^{2-}$ complex, the complex formation of Cd (II) ions with the ligand has been decreased.

3.4. Selective adsorption

For the selective adsorption experiment, a mixed solution contained Cd(II), Zn(II), Cu(II), Pb(II), Ni(II), Mn(II), and Co(II) ($C_{initial}$ = 100 mg L^{-1}, 100 mL) and the pH value of the solution kept 9.0 ± 0.1. The adsorption process on the Br-PADAP/SBA-15 (30 mg) was conducted for 90 min. Fig. 8 shows the selective sorption of divalent heavy metal ions (Cd, Zn, Cu, Pb, Ni, Mn, and Co) onto Br-PADAP/SBA-15. For Cd(II) ions, about 96% removal efficiency is observed. Both Co(II) and Zn(II) ions show more than 4% removal efficiency while Cu, Pb, Ni, and Mn ions exhibit only slight adsorption.

Obviously, Cd(II) ions can be preferentially removed from the mixed metal ions aqueous solution. Because of the difference in stability constant, chelation ability, the selective adsorption on the Br-PADAP/SBA-15 might happen in a competitive environment. Maybe this is why Cd(II) was adsorbed preferably.

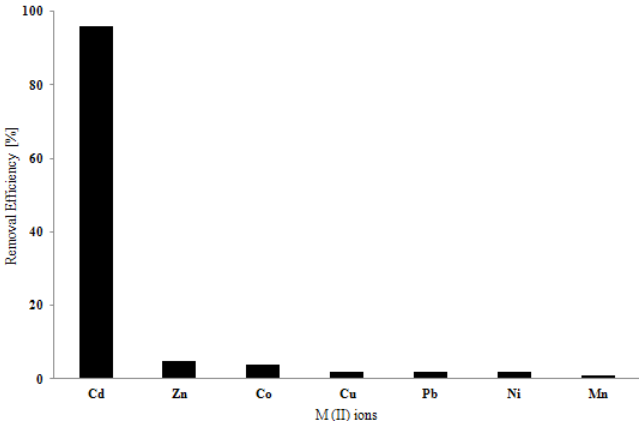

Fig. 8. Metal ions removal on the Br-PADAP/SBA-15 from a mixed solution of metal ions ($C_{initial}$ = 100 mg L^{-1}, pH = 9.0, and $t_{adsorption}$ = 90 min).

3.5. Desorption studies

To distinguishing the reuse capability of the adsorbent after Cd(II) adsorption, its surface was stripped using HNO_3. To optimization of the amount of the acid that is needed toward quantifiable stripping of the burdened Cd(II), some experiments were done with changing concentrations of HNO_3 in the range 0.01–1 M, where effectual desorption could be attained using 0.2 M HNO_3. Composite loaded with Cd(II) was placed in the 0.2 M HNO_3 and stirred at 100 rpm for 20 min and the final Cd(II) concentration was determined. After each cycle, the used adsorbent was washed well with distilled water and used in the succeeding cycle. The desorbed amount was calculated from subtraction of the final Cd(II) concentration in the stripping medium from the value of Cd ions loaded on the nanocomposite. After consecutive leaching, the sample can reuse six times using 30 mg of the composite and 100 mg L^{-1} of Cd(II) solution in the total volume of 100 mL. 98.0% of the Cd(II) was removed in the first cycle. Adsorbed Cd(II) could be stripped in 20 min by the introducing of H^+ that contested with Cd(II) ions for binding sites. The utilized nanocomposite was treated with 0.2 M HNO_3 which caused to 96.7% stripping of Cd(II). In the second cycle, the material removed 96% of Cd(II) that could be desorbed up to 94.8%. In the third cycle, 91% adsorption and 89.5% desorption were found. A considerable decrease in the removal can be found in the fourth cycle signifying the profit efficiency of the adsorbent. It was found that the adsorbent can eliminate 68% Cd(II) and desorption of 61.3% in the sixth cycle.

3.6. Adsorption isotherm study

In order to gain a better understanding of sorption mechanisms and evaluate the sorption performance, achieved data for cadmium ions adsorption onto Br-PADAP/SBA-15 were analyzed by means of the Langmuir and Freundlich isotherm models.

3.6.1. The Langmuir isotherm model

Langmuir theory is based on the hypothesis that the application of adsorbate happens on a homogeneous surface by monolayer adsorption and adsorption energy is persistent in this model. The theory is shown by the subsequent equation:

$$q_e = \frac{q_m k_L C_e}{1 + k_L C_e} \tag{1}$$

where q_e is the amount of cadmium adsorbed (mg g^{-1}) at equilibrium, C_e is the equilibrium cadmium quantity (mg L^{-1}), and k_L (L mg^{-1}) and q_m (mg g^{-1}) are the Langmuir constants. Table 2 shows the predicted isotherm constants (k_L and q_m) and the corresponding R^2 values. Four dissimilar linearized Langmuir isotherms can be gotten.

Type 1 Langmuir isotherm (Fig. 9) is found as the finest fitting linearized Langmuir expression ($R^2 \approx 1$). Therefore, the results were taken from Langmuir equation type 1. Correlation coefficients are near to 1 which means that experimental data fitted in this model well.

Crucial characteristics of the Langmuir type adsorption could be defined by a term "R_L" as dimension-less constant separation factor (see Table 2). The R_L value could be defined as follow:

$$R_L = \frac{1}{1 + k_L C_0} \tag{2}$$

where C_0 is the initial concentration of cadmium solution (mg L^{-1}), k_L is the Langmuir constant (L mg^{-1}), and the parameter R_L designates the shape of the isotherm consequently. The magnitude of the exponent R_L springs an indication of the favorability of adsorption. According to the data achieved for R_L in Table 2, those values represent favorable adsorption conditions.

3.6.2. Freundlich isotherm model

The Freundlich isotherm model equation deals with physicochemical adsorption on the heterogeneous surface at sites with different energy of adsorption and with non-identical adsorption sites, which are not always available. Mathematically, it is characterized by Eq. (3) as follows:

$$q_e = k_F C_e^{1/n} \tag{3}$$

where K_F is the Freundlich constant and n is the heterogeneity factor. The K_F value is attributed to the adsorption

Table 2
Calculated Langmuir isotherm parameters by different linear method

Langmuir adsorption isotherm	Type 1	Type 2	Type 3	Type 4
q_m	5,000.0	3,333.3	4,036.3	5,288.0
K_L	0.1333	0.4286	0.3374	0.1185
R^2	0.9967	0.7584	0.5151	0.6444
R_L	0.0698	0.0228	0.0289	0.0778

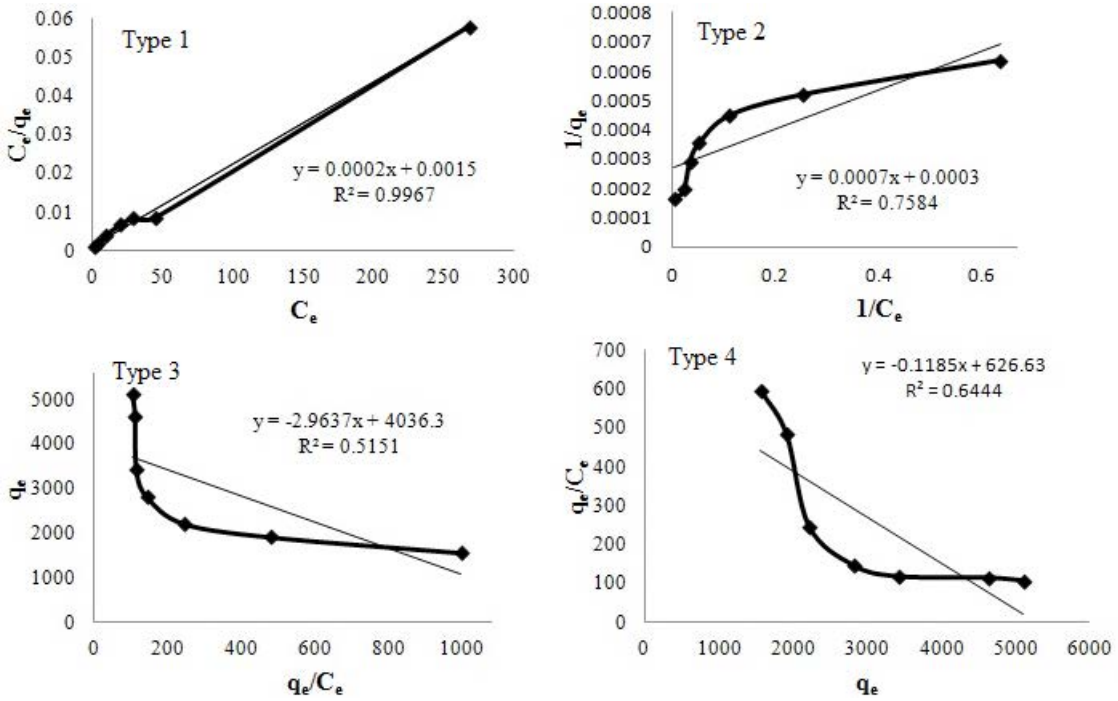

Fig. 9. Removal of Cd(II) ions with: Br-PADAP/SBA-15 (the initial concentration, pH value, and solution volume and adsorbent quantity were 100 mg L^{-1}, 9, 100 mL, and 0.03 g, respectively), Langmuir isotherm models.

capacity, while 1/*n* value is related to the adsorption intensity. The linear form could represent the Freundlich model as follow:

$$\ln q_e = \ln k_F + 1/n \ln C_e \quad (4)$$

Therefore, K_F and 1/*n* could be distinguished from the linear plot of ln q_e against ln C_e. The K_F and *n* values are listed in Table 3. The R^2 value is below 0.95 signifying that the data of adsorption is not close-fitting to this model. The value of correlation coefficient is lower than the other three isotherms values. Despite correlation coefficient of 0.9051 in Freundlich isotherm (see Fig. 10) is not great, however, it represents the poorer fit of experimental data than the other isotherms.

The fitting of the data, obtained from the sorption of Cd(II) ions on Br-PADAP/SBA-15, to the two isotherm models showed that the linearity of the Langmuir isotherm type 1 model (r^2 = 0.9967) was higher than that of the other isotherm models (Table 3). It shows that the sorption of Cd(II) ions on Br-PADAP/SBA-15 was one layered and took place in specific spots of homogeneous N and O atoms on the sorption surface of the Br-PADAP.

3.7. Adsorption kinetics study

The rapid adsorption attributes to plenty of N and O atoms within Br-PADAP and sponge-like porous structure of SBA-15 adsorbent that increase adsorption sites for Cd(II) adsorption. The pseudo-first-order and pseudo-second-order models were analyzed to designate the adsorption kinetics of this study.

Table 3
Calculated isotherm parameters of two models by linear method

Langmuir isotherm model				Freundlich isotherm model		
q_m	k_L	R_L	R^2	K_F	*n*	R^2
5,000.0	0.1333	0.0698	0.9967	1,435.8	4.219	0.9051

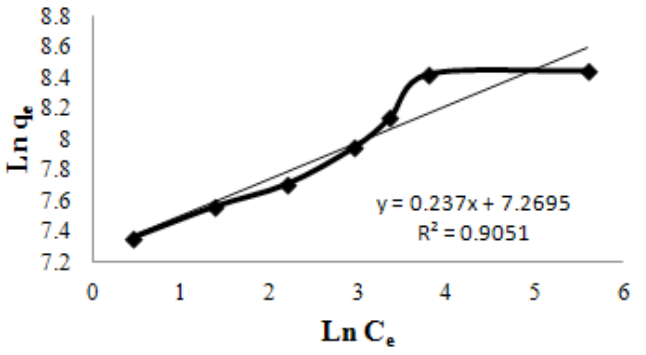

Fig. 10. Removal of Cd(II) ions with: Br-PADAP/SBA-15 (the initial concentration, pH value, and solution volume and adsorbent quantity were 100 mg L^{-1}, 9, 100 mL, and 0.03 g, respectively), Freundlich isotherm.

3.7.1. Pseudo-first-order

An easy kinetic analysis of adsorption is provided by a pseudo-first-order equation that describes the kinetics of the adsorption process as follow:

$$\frac{dq_t}{dt} = k_1(q_e - q_t) \quad (5)$$

where k_1 is the rate constant of pseudo-first-order adsorption (min^{-1}), and q_e and q_t are the amount of Cd adsorbed on Br-PADAP/SBA-15 (mg g^{-1}) at equilibrium and at time t, respectively. Following confident integration by using the initial conditions $q_t = 0$ at $t = 0$ and $q_t = q_t$ at $t = t$, Eq. (6) is changed as below:

$$\ln (q_e - q_t) = \ln q_e - k_1 t \quad (6)$$

Linear plot feature of $\ln (q_e - q_t)$ against t (see Fig. 11(a)) for adsorption of Cd(II) ions on Br-PADAP/SBA-15 was achieved and the k_1 and q_e values calculated from slope and intercept of this line were summarized in Table 4.

3.7.2. Pseudo-second-order

The pseudo-second-order rate expression is based on the adsorption equilibrium capacity and can be expressed with Eq. (7) and presented linearly by the Eq. (8):

$$\frac{dq_t}{dt} = k_2 (q_e - q_t)^2 \quad (7)$$

$$\frac{t}{d_t} = \frac{1}{k_2 q_e^2} + \frac{1}{q_e} t \quad (8)$$

In Eq. (7), k_2 is the rate constant of pseudo-second-order adsorption (g mg^{-1} min), q_e and q_t are the amount of Cd adsorbed on Br-PADAP/SBA-15 (mg g^{-1}) at equilibrium and at time t, correspondingly. Linear plot feature of t/q_t against t (see Fig. 11(b)) for adsorption of Cd(II) on Br-PADAP/SBA-15 was achieved and the k_2 and q_e values calculated from the slope and line intercept were summarized in Table 4. The adsorption kinetics is more aligned with the pseudo-second-order model due to the higher correlation coefficient (R^2) than the pseudo-first-order model.

Table 4
Constants for the kinetic sorption data using two models

$q_{e,exp}$ (mg g^{-1})	Pseudo-first-order			Pseudo-second-order		
	K_1 (min^{-1})	$q_{e,Cal}$ (mg g^{-1})	R^2	K_2 (g mg^{-1} min)	$q_{e,Cal}$ (mg g^{-1})	R^2
5,000.0	0.0337	878.8	0.9895	0.00006	2,000.0	0.9972

3.8. Gibbs free energy, enthalpy, and entropy

The Gibbs free energy changes ($\Delta G°$) were determined using the following Eq. (9):

$$-\Delta G° = RT \ln K \quad (9)$$

where R is the gas global constant, T is the absolute temperature, and K is the partition ratio. The values of the equilibrium constant (K) and Gibbs free energy change ($\Delta G°$) are shown in Table 5. The negative value of $\Delta G°$ confirms that the adsorption of Cd(II) ions onto Br-PADAP/SBA-15 is spontaneous and thermodynamically favorable. By increase in temperature, the $\Delta G°$ value decreases, causing in lower adsorption capacity. Standard enthalpy ($\Delta H°$) and entropy ($\Delta S°$) were determined from the Van't Hoff Eq. (10) as follows:

$$\ln K = \frac{\Delta S°}{R} - \frac{\Delta H°}{RT} \quad (10)$$

$\Delta H°$ and $\Delta S°$ were calculated from the slope and intercept of the plot of ln K against $1/T$, as shown in Fig. 12.

The values of $\Delta H°$ and $\Delta S°$ are listed in Table 5. The positive value of $\Delta H°$ points to the endothermic nature of adsorption.

Table 5
Thermodynamic parameters ($\Delta H°$, $\Delta G°$, $\Delta S°$) for the adsorption of Cd(II) ions on Br-PADAP/SBA-15

Temperature (°C)	K	$\Delta G°$ (kJ mol^{-1})	$\Delta H°$ (kJ mol^{-1})	$\Delta S°$ (J mol^{-1} K)	R^2
25	115.01	–11.762	6.614	61.634	0.9991
35	125.34	–12.377			
45	136.05	–12.995			

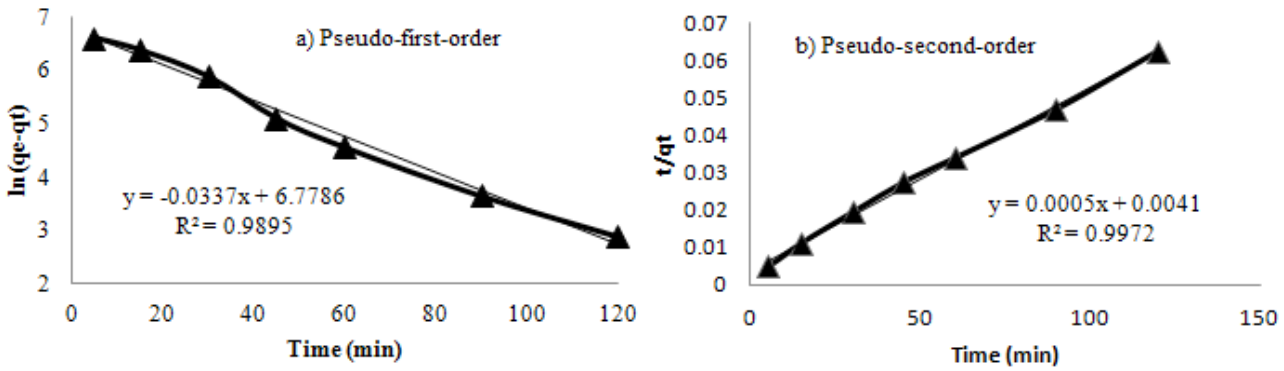

Fig. 11. Removal of Cd(II) with: Br-PADAP/SBA-15 (the initial concentration, pH, volume of solution and amount of adsorbent were 100 mg L^{-1}, 9, 100 mL, and 0.03 g, respectively), (a) Pseudo-first-order, (b) Pseudo-second-order.

3.9. Comparison with other studies

Although a direct comparison between two different adsorbents is difficult due to the different experimental conditions, q_m (mg g^{-1}), an isotherm parameter or sorption capacity, has been commonly used to evaluate and comparison of adsorption capability. A high q_m is desirable for an excellent adsorbent. Table 6 lists the Cd(II) adsorption capacities on Br-PADAP/SBA-15 and some commonly used adsorbents such as graphene, chitosan, sepiolite, silica materials, PS-GO gel, and graphene oxide nanosheets. According to Langmuir isotherm equation, the calculated maximum uptake capacities (q_m) of Cd(II) on Br-PADAP/SBA-15 is 5,000.0 mg g^{-1}; that is much higher than those on the reported adsorbents. Additionally, if we take into account, the particular characteristics of the SBA-15 support (excellent textural properties, high hydrophilicity, and their surface silanol groups that can be easily functionalized by using various organic species), we can conclude that modified SBA-15 mesoporous silica is an interesting candidate for applications in heavy metal removal from wastewater.

3.10. Removing of Cd(II) ions from water and wastewater samples

Firstly, according to Table 7, some real water and wastewater samples (100 mL) were prepared and filtered using a 0.45-mm pore size membrane filter before any analysis to remove any suspended particles. In addition, the real concentration of Cd(II) ions in wastewater samples, after filtration was determined by FAAS. As shown in Table 7, high removal percent is achieved for each real sample, suggesting the proposed method could be applied successfully for the removing of Cd(II) ions in water and wastewater samples.

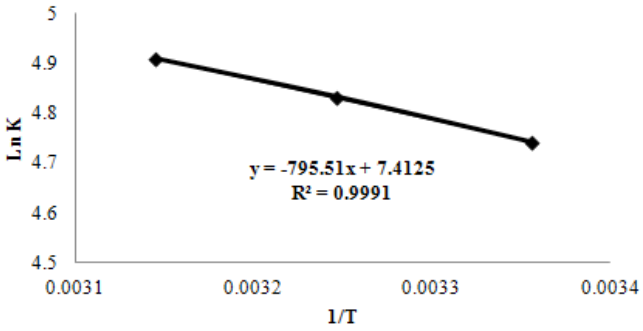

Fig. 12. Removal of Cd(II) ions with: Br-PADAP/SBA-15 (the initial concentration, pH, and volume of solution and amount of adsorbent were 100 mg L^{-1}, 9, 100 mL, and 0.03 g, respectively), Van't Hoff Regression.

4. Conclusion

An effective adsorbent for removal of cadmium ions has been prepared by immobilization of Br-PADAP on the surface of the SBA-15 mesoporous silica. The modified SBA-15 mesoporous silica adsorbent has unique advantages over commonly used sorbents because of its low cost, high adsorptivity, and reusability. Cadmium ions were completely removed at pH 9 after stirring for 90 min. The functionalized SBA-15 presented developed adsorption selectivity for Cd(II) ions compared with other metal ions existing in the mixture solution. These consequences propose the probability of using this adsorbent in the selective recovery of the Cd(II) ions from a mixed metal ions solution. The Br-PADAP/SBA-15 can be reused up to six cycles making this approach very economical. The equilibrium sorption capacity of 5,000.0 mg g^{-1} as determined from the

Table 7
Removal of Cd(II) ions from water and wastewater samples

Water and wastewater samples	concentration of Cd(II) (mg L^{-1})	Removal (%)
Sea water[a]	1.20 ± 0.04	97 ± 1.5
River water[b]	0.30 ± 0.01	98 ± 1.2
wastewater of power station[c]	21.40 ± 0.40	96 ± 0.9
wastewater of hospital[d]	6.00 ± 0.09	96 ± 1.3
wastewater of slaughterhouse[e]	2.10 ± 0.07	97 ± 1.6
wastewater of MDF factory[f]	17.50 ± 0.30	95 ± 0.8

[a]Caspian seawater, Iran.
[b]Siahrood River, Qaemshahr, Iran.
[c]Electrical Power Station, Neka, Mazandaran, Iran.
[d]Bu-Ali sina Hospital, Sari, Iran.
[e]Cattle Slaughterhouse, Sari, Iran.
[f]Arian Chemistry Company, Sari, Iran.

Table 6
Comparison of the maximum uptake of Cd(II) ions on various adsorbents.

Adsorbent	q_m (mg g^{-1})	C_o (mg L^{-1})	pH	Temperature (K)	Ref.
Amino functionalized graphene	27.95	5	6–7	298	[41]
Modified kaolinite	36.47	400	5	293	[42]
Mercator functionalized sepiolite	34.84	–	–	298	[43]
Ethylenediamine/SBA-15	100.04	2	4.5	298	[44]
2-mercaptopyrimidine/SBA-15	111.28	1,124	6	298	[23]
PS-GO gel	136.98	10	6	313	[45]
Amino functionalized silica	190.5	50	6	298	[46]
Guar-graft-poly-silica composite	2,000.0	500	9	303	[47]
Graphene oxide nanosheets	106.3	20	6	303	[48]
Br-PADAP/SBA-15	5,000.0	100	9	298	This work

Langmuir isotherm is very high compared with the previously reported adsorbents. The Br-PADAP/SBA-15 exhibits an outstanding ability to remove cadmium from aqueous solutions. The adsorption data fit better with Langmuir adsorption isotherm representing surface homogeneity as well as monolayer adsorption. The kinetic study of the adsorption of Cd(II) ion onto Br-PADAP/SBA-15 was performed and it was found that the second-order kinetic model fits better with the data. The study concludes that the Br-PADAP/SBA-15 could be employed as a low-cost adsorbent, as an alternative to commercial adsorbents for the removal of metal ions in practical applications. The mesoporous Br-PADAP/SBA-15 may be promising candidate toward removal of heavy metals.

Acknowledgment

Financial support of Islamic Azad University of Qaemshahr is highly appreciated.

References

[1] A. Yazdankhah, S.E. Moradi, S. Amirmahmoodi, M. Abbasian, S. Esmaeily Shoja, Enhanced sorption of cadmium ion on highly ordered nanoporous carbon by using different surfactant modification, Microporous Mesoporous Mater., 133 (2010) 45–53.
[2] R.E. Cameron, Guide to Site and Soil Description for Hazardous Waste Site Characterization, Vol. 1: Metals, Environmental Protection Agency (EPA), Washington, DC, 1992.
[3] Organisation for Economic Co-operation and Development (OECD), Risk Reduction Monograph No. 5: Cadmium OECD Environment Directorate, Paris, France, 1994.
[4] M.P. Waalkes, Cadmium carcinogenesis in review, review, J. Inorg. Biochem., 79 (2000) 241–244.
[5] S. Cay, A. Uyanik, A. Ozasik, Single and binary component adsorption of copper (II) and cadmium (II) from aqueous solutions using tea-industry waste, Sep. Purif. Technol., 38 (2004) 273–280.
[6] National Library of Medicine, Hazardous Substances Data Bank (HSDB), 1996.
[7] J. De Zuane, Handbook of Drinking Water Quality Standards and Controls, Van Nostrand Reinhold, New York, 1990, pp. 64–69.
[8] C.W. Cheung, J.F. Porter, G. Mckay, Adsorption kinetic analysis for the removal of cadmium ions from effluents using bone char, Water Res., 35 (2001) 605–612.
[9] H. Serencam, A. Gundogdu, Y. Uygur, B. Kemer, V.N. Bulut, C. Duran, M. Soylak, M. Tufekci, Removal of cadmium from aqueous solution by Nordmann fir (*Abies nordmanniana* (Stev.) Spach. Subsp. *nordmanniana*) leaves, Bioresour. Technol., 99 (2008) 1992–2000.
[10] M. Ghaedi, S. Hajati, B. Barazesh, F. Karimi, G. Ghezelbash, *Saccharomyces cerevisiae* for the biosorption of basic dyes from binary component systems and the high order derivative spectrophotometric method for simultaneous analysis of Brilliant green and Methylene blue, J. Ind. Eng. Chem., 19 (2013) 227–233.
[11] J. Labanda, J. Sabate, J. Llorens, Experimental and modeling study of the adsorption of single and binary dye solutions with an ion-exchange membrane adsorber, Chem. Eng. J., 166 (2011) 536–543.
[12] Y. Huang, D. Wu, X. Wang, W. Huang, D. Lawless, X. Feng, Removal of heavy metals from water using polyvinylamine by polymer-enhanced ultrafiltration and flocculation, Sep. Purif. Technol., 158 (2016) 124–136.
[13] A. Cincotti, A. Mameli, A.M. Locci, R. Orru, G. Cao, Heavy metals uptake by sardinian natural zeolites: experiment and modeling, Ind. Eng. Chem. Res., 45 (2006) 1074–1084.
[14] S.M. Lee, D. Tiwari, Organo and inorgano-organo-modified clays in the remediation of aqueous solutions: an overview, Appl. Clay Sci. 59–60 (2012) 84–102.
[15] L. Yan, Y. Huang, J.L. Cui, C.Y. Jing, Simultaneous As (III) and Cd removal from copper smelting wastewater using granular TiO_2 columns, Water Res. 68 (2015) 572–579.
[16] R. Xuemei, Q. Wu, H. Xu, D. Shao, X. Tan, W. Shi, C. Chen, J. Li, Z. Chai, T. Hayat, X. Wang, New insight into GO, cadmium (II), phosphate interaction and its role in GO colloidal behavior, Environ. Sci. Technol., 50 (2016) 9361–9369.
[17] X. Dong, C. Wang, H. Li, M. Wu, S. Liao, D. Zhang, B. Pan, The sorption of heavy metals on thermally treated sediments with high organic matter content, Bioresour. Technol., 160 (2014) 123–128.
[18] P.K. Jal, S. Patel, B.K. Mishra, Chemical modification of silica surface by immobilization of functional groups for extractive concentration of metal ions, Talanta, 62 (2004) 1005–1028.
[19] A. Mirabi, Z. Dalirandeh, A. Shokuhi-Rad, Preparation of modified magnetic nanoparticles as asorbent for the preconcentration and determination of cadmium ions in food and environmental water samples prior to flame atomicabsorption spectrometry, J. Magn. Magn. Mater., 381 (2015) 138–144.
[20] A. Mirabi, A. Shokouhi-Rad, S. Nourani, Application of modified magnetic nanoparticles as a sorbent for preconcentration and determination of nickel ions in food and environmental water samples, TrAC Trends Anal. Chem., 74 (2015) 146–151.
[21] A. Mirabi, A. Shokuhi-Rad, H. Khodadad, Modified surface based on magnetic nanocomposite of dithiooxamide/Fe3O4 as a sorbent for preconcentration and determination of trace amounts of copper, J. Magn. Magn. Mater., 389 (2015) 130–135.
[22] A. Mirabi, A. Shokuhi-Rad, M.R. Jamali, N. Danesh, Use of modified γ-alumina nanoparticles for the extraction and preconcentration of trace amounts of cadmium ions, Aust. J. Chem., 69 (2016) 314–318.
[23] D. Perez-Quintanilla, I. del Hierro, M. Fajardo, I. Sierra, Adsorption of cadmium(II) from aqueous media onto a mesoporous silica chemically modified with 2-mercaptopyrimidine, J. Mater. Chem., 16 (2006) 1757–1764.
[24] D. Zareyee, S.R. Tuyehdarvary, L. Allahgholipour, Z. Hossaini, M.A. Khalilzadeh, Catalytic performance of hydrophobic sulfonated nanocatalysts CMK-5-SO3H and SBA-15-Ph-PrSO3H for ecofriendly synthesis of 2-substituted benzimidazoles in water, Synlett, 27 (2016) 1251–1254.
[25] D. Zareyee, A.R. Ghadikolaee, M.A. Khalilzadeh, Highly efficient solvent-free acetylation of alcohols with acetic anhydride catalyzed by recyclable sulfonic acid catalyst (SBA-15–Ph–Pr–SO3H)—an environmentally benign method, Can. J. Chem., 90 (2012) 464–468.
[26] D. Zareyee, R. Asghari, M.A. Khalilzadeh, Silylation of alcohols and phenols with hexamethyldisilazane over highly reusable propyl sulfonic acid functionalized nanostructured SBA-15, Chinese J. Catal., 32(2011) 1864–1868.
[27] V.B. Cashin, D.S. Eldridge, A. Yu, D. Zhao, Surface functionalization and manipulation of mesoporous silica adsorbents for improved removal of pollutants: a review, Environ. Sci. Water Res. Technol., 4 (2018) 110–128.
[28] Y. Zhu, Z. Cheng, Q. Xiang, Y. Zhu, J. Xu, Rational design and synthesis of aldehyde-functionalized mesoporous SBA-15 for high-performance ammonia sensor, Sens. Actuators, B. 256 (2018) 888–895.
[29] I. Yuranov, L. Kiwi-Minsker, P. Buffat, A. Renken, Selective synthesis of Pd nanoparticles in complementary micropores of SBA-15, Chem. Mater., 16 (2004) 760–761.
[30] A.Y. Khodakov, V.L. Zholobenko, R. Bechara, D. Durand, Impact of aqueous impregnation on the long-range ordering and mesoporous structure of cobalt containing MCM-41 and SBA-15 materials, Microporous Mesoporous Mater., 79 (2005) 29–39.
[31] S.G. de-Avila, L.C.C. Silva, J.R. Matos, Optimisation of SBA-15 properties using Soxhlet solvent extraction for template removal, Microporous Mesoporous Mater., 234 (2016) 277–286.

[32] Y. Yamini, J. Hassan, R. Mohandesi, N. Bahramifar, Preconcentration of trace amounts of beryllium in water samples on octadecyl silica cartridges modified by quinalizarine and its determination with atomic absorption spectrometry. Talanta, 56 (2002) 375–381.
[33] V.K. Gupta, P. Singh, N. Rahman, Adsorption behavior of Hg(II), Pb(II), and Cd(II) from aqueous solution on Duolite C-433: a synthetic resin, J. Colloid Interf. Sci. 275 (2004) 398–402.
[34] A.A. Atia, A.M. Donia, K.Z. Elwakeel, Adsorption behaviour of non-transition metal ions on a synthetic chelating resin bearing iminoacetate functions, Sep. Purif. Technol., 43 (2005) 43–48.
[35] A. Demirbas, E. Pehlivan, F. Gode, T. Altun, G. Arslan, Adsorption of Cu(II), Zn(II), Ni(II), Pb(II), and Cd(II) from aqueous solution on Amberlite IR-120 synthetic resin, J. Colloid Interf. Sci., 282 (2005) 20–25.
[36] V.D. Grebenyuk, S.V. Verbich, N.A. Linkov, V.M. Linkov, Adsorption of heavy metal ions by aminocarboxyl ion exchanger ANKB-35, Desalination, 115 (1998) 239–254.
[37] B. Salih, A. Denizli, C. Kavaklı, R. Say, E. Piskin, Adsorption of heavy metal ions onto dithizone-anchored poly (EGDMA-HEMA) microbeads, Talanta, 46 (1998) 1205–1213.
[38] A.A. Atia, A.M. Donia, A.M. Yousif, Synthesis of amine and thio chelating resins and study of their interaction with zinc(II), cadmium(II) and mercury(II) ions in their aqueous solutions, React. Funct. Polym., 56 (2003) 75–82.
[39] A. Mirabi, A. Shokuhi-Rad, Z. Khanjari, M. Moradian, Preparation of SBA-15/graphene oxide nanocomposites forpreconcentration and determination of trace amounts of rutoside inblood plasma and urine, Sens. Actuators, B., 253 (2017) 533–541.
[40] A. Mirabi, S.N. Hosseini, Use of modified nanosorbent materials for extraction and determination of trace amounts of copper ions in food and natural water samples, Trends Appl. Sci. Res., 7 (2012) 541–549.
[41] X.Y. Guo, B. Du, Q. Wei, J. Yang, L. Hu, L. Yan, W. Xu, Synthesis of amino functionalized magnetic graphenes composite material and its application to remove Cr(VI), Pb(II), Hg(II), Cd(II) and Ni(II) from contaminated water, J. Hazard. Mater., 278 (2014) 211–220.
[42] A. Sari, M. Tuzen, Cd(II) adsorption from aqueous solution by raw and modified kaolinite, Appl. Clay Sci., 88–89 (2014) 63–72.
[43] X. Liang, Y. Xu, G. Sun, L. Wang, Y. Sun, Y. Sun, X. Qin, Preparation and characterization of mercapto functionalized sepiolite and their application for sorption of lead and cadmium, Chem. Eng. J., 174 (2011) 436–444.
[44] L. Hajiaghababaei, A. Badiei, M.R. Ganjali, S. Heydari, Y. Khaniani, Gh. Mohammadi-Ziarani, Highly efficient removal and preconcentration of lead and cadmium cations from water and wastewater samples using ethylenediamine functionalized SBA-15, Desalination, 266 (2011) 182–187.
[45] G. Zhou, C. Liu, Y. Tang, S. Luo, Z. Zeng, Y. Liu, R. Xu, L. Chu, Sponge-like polysiloxane-graphene oxide gel as a highly efficient and renewable adsorbent for lead and cadmium metals removal from wastewater, Chem. Eng. J., 280 (2015) 275–282.
[46] A.M. El-Toni, M.A. Habila, M.A. Ibrahim, J.P. Labis, Z.A. Alothman, Simple and facile synthesis of amino functionalized hollow core-mesoporous shell silica spheres using anionic surfactant for Pb(II), Cd(II), and Zn(II) adsorption and recovery, Chem. Eng. J., 251 (2014) 441–451.
[47] V. Singh, S. Pandey, S.K. Singh, R. Sanghi, Removal of cadmium from aqueous solutions by adsorption using poly (acrylamide) modified guar gum–silica nanocomposites, Sep. Purif. Technol., 67 (2009) 251–261.
[48] G. Zhao, J. Li, X. Ren, C. Chen, X. Wang, Few-layered graphene oxide nanosheets as superior sorbents for heavy metal ion pollution management, Environ. Sci. Technol., 45(2011) 10454–10462.